DOI: 10.1478/AAPP.98S1A5

AAPP | Atti della Accademia Peloritana dei Pericolanti
Classe di Scienze Fisiche, Matematiche e Naturali
ISSN 1825-1242

Vol. 98, No. S1, A5 (2020)

RAMAN AND BRILLOUIN SCATTERING OF SPHERICAL NANOPARTICLES AND THEIR CLUSTERS

MARIA SECCHI [a] AND MAURIZIO MONTAGNA [b *]

ABSTRACT. The inelastic light scattering of the acoustic vibration of spherical nanoparticles is reviewed. For particles much smaller than the wavelength of the exciting light (λ), with a diameter (d) smaller than about 20 nm, the dominant physical mechanism, called Raman, is the polarizability fluctuation due to dipole dipole or bond polarizability induced effects. Only spheroidal modes with $l = 0$ and $l = 2$ are Raman active. For particles of size comparable with λ (d larger than about 100 nm) a different physical mechanism is dominant, the mass displacement and relative polarization associated with the vibration, as for the usual Brillouin scattering of liquid and solids. As the size increases, higher and higher l modes with higher and higher n, the index that labels the radial wavevector, become important and many dozen of peaks appear for $d > 500$ nm. A simple model allows to reproduce the main features of the observed spectra. A more precise agreement is obtained by a refinement that considers the interaction among the particles in a phononic crystals. The interaction produces broadening and shift of the lines and accounts for the presence of a very low frequency broad band, attributed to the density of states of the modes of the sound propagation in the crystal. The analysis of the spectra allows to obtain information on the dynamics of the single free sphere and on the strength of the interaction. By measuring the temperature-dependence of the Brillouin spectra in clusters of polystyrene nanoparticles during the sintering process, it is possible to identify the glass-transition temperature and calculate the elastic modulus of individual nanoparticles as a function of particle size and chemistry. Surface mobility is evidenced by a size dependence of the interaction among the particles and of the glass transition temperature.

1. Introduction

After the first works on silver colloids in alkali halides (Rzepka *et al.* 1981) and on spinel nanocrystals in cordierite glasses (Duval *et al.* 1986), low frequency Raman scattering from symmetric and quadrupolar acoustic vibrations has become a method to study many composite systems containing metallic, insulator or semiconductor nanoparticles (NPs) and to determine the size of the particles. Few peaks in the range 3-50 cm^{-1} were observed (Duval *et al.* 1986; Champagnon *et al.* 1987; Malinovsky *et al.* 1988; Mariotto *et al.* 1988; Abel 1990; Capobianco *et al.* 1991; Fujii *et al.* 1991; Champagnon *et al.* 1993; Tanaka *et al.* 1993; Ferrari *et al.* 1996; Fujii *et al.* 1996; Zi *et al.* 1998; Ivanda *et al.* 1999; Palpant *et al.*

1999a,b; Zhao and Masumoto 1999; Gangopadhyay *et al.* 2000; Irmer *et al.* 2000; Verma *et al.* 2000; Bottani *et al.* 2001; Ceccato *et al.* 2001; Duval *et al.* 2001; Wu *et al.* 2001; Cataliotti *et al.* 2002; Tikhomirov *et al.* 2002; Ivanda *et al.* 2003; Montagna *et al.* 2003; Bachelier and Mlayah 2004; Saviot *et al.* 2004; Yang *et al.* 2005; Bragas *et al.* 2006; Ivanda *et al.* 2006; Jestin *et al.* 2006; Bachelier *et al.* 2007; Murray *et al.* 2007; Gupta *et al.* 2008; Kostic *et al.* 2008; Ristic *et al.* 2009; Chen *et al.* 2010; Mikac *et al.* 2011; Mankad *et al.* 2012; Mohapatra *et al.* 2012; Mankad *et al.* 2013; Zatryb *et al.* 2015; Mork *et al.* 2016; Simon *et al.* 2016; Girard *et al.* 2017; Lee *et al.* 2017).

All the above cited experiments were performed on systems formed by very small particles of size $qd \ll 1$, where d is the diameter of the particle and q is the exchanged wavevector of the light. In fact, the theoretical results were derived in the hypothesis that the fields, scattered by different polarizable units within the particle, are all in phase, $qd \ll 1$. Later, a different phenomenology was observed in light scattering experiments from particles with sizes of hundreds of nanometers (Kuok *et al.* 2003a,b). The particles were made up of sol-gel derived silica, polystyrene or PMMA, aggregated to form 3D photonic crystals. The low frequency spectra of these systems, and those relative to a single particle (Li *et al.* 2006), exhibit many peaks with comparable intensities. The peaks were attributed to the spheroidal (s,n,l) acoustic vibrations confined in a single sphere.

Three different steps are clearly present in the evolution of the analysis of the Brillouin spectra in phononic crystals. The first attempt was to use a model for the calculation of the Brillouin intensity, for assigning the observed peaks to the modes of an isolated NP (Montagna 2008a; Still *et al.* 2010). Later, it was recognized that particle–particle interactions in clusters of NPs influence the eigenfrequencies of individual NPs and lead to a low frequency broad band, which is attributed to the propagation of longitudinal waves (Mattarelli *et al.* 2012, 2013). More recently, it has been shown that the light scattering experiments can be used to follow the process of sintering of NP (Saviot *et al.* 2017; Kim *et al.* 2018).

Here, we will briefly review the three steps and show how the technique can be used to study the effect of nano-confinement of the acoustic-like vibrations. For polymeric particles, it has been suggested the existence of a surface layer with higher mobility of the chains (Kim *et al.* 2018). The role of this mobile surface layer is more important as the particles are small, resulting in a size dependent glass transition temperature, measurable by Brillouin Scattering (BS).

2. Vibrations of a free sphere

The dynamics of a homogeneous elastic sphere with a free surface was studied by Lamb, who gave frequencies and displacement patterns as a function of the elastic constants and density (Lamb 1881). The vibrations are grouped into two categories, the torsional and the spheroidal ones. The former involve only shear motions and do not change the volume of the sphere, the latter involve both shear and stretching motions and produce radial displacement. Torsional and spheroidal modes are classified according to the symmetry group of the sphere by the labels (l,m) as for the spherical harmonic functions Y_l^m. The symmetric $l = 0$ spheroidal modes have a purely radial pattern with spherical symmetry. At higher l values, angular corrugation appears: l measures the number of wavelengths along a circle on the

surface. A third index ($n = 1,2,..$) labels the sequence of eigenmodes, in increasing order of frequency and radial wavevector, at fixed angular shape (l,m). We will use the notation (p,n,l,m) with $p = s,t$ for spheroidal and torsional modes, respectively. All modes have frequencies f that scale inversely to the spherical diameter d (Lamb 1881):

$$f(p,n,l) = A(p,n,l)v_L/d \tag{1}$$

where $A(p,n,l)$ are dimensionless quantities of the order of one that depend on the ratio between the transverse (v_T) and longitudinal (v_L) sound velocities in the particle. Typical frequencies are in the range of THz for spheres of few nanometers and of GHz for spheres in the range of micrometers. Figure 1 shows some low frequency Lamb modes.

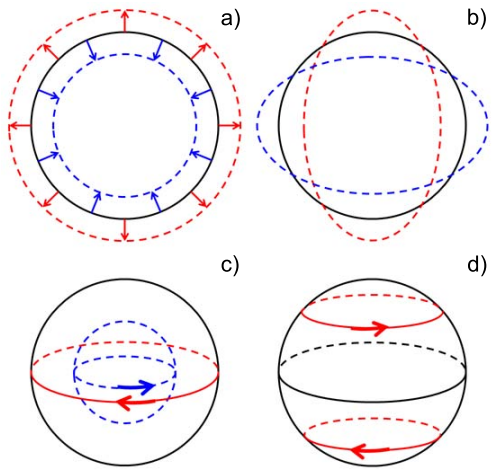

FIGURE 1. Schematic representation of low frequency Lamb modes: (a) the spheroidal symmetric mode, $(s,1,0)$, (b) the spheroidal quadrupolar mode, $(s,1,2,0)$, (c) the torsional mode $(t,2,1,0)$, and (d) the torsional mode $(t,1,2,0)$.

The spheroidal symmetric mode $(s,1,0)$ is shown in Fig. 1a. Its frequency depends on both transverse and longitudinal sound velocity. The five degenerate spheroidal quadrupolar $(s,1,2,m)$ modes transform the sphere, alternated in time, in a prolate and oblate ellipsoid, as shown in Fig. 1b. The three $(s,1,1,m)$ modes, not shown, are zero frequency rigid translations along three normal axes (m=x, y, z). Figure 1c shows the displacement pattern of one of the three degenerate $(t,2,1,m)$ with counter rotations of the external and internal parts of the sphere. The $(t,1,1,m)$, not shown, are zero frequency rigid rotations. Figure 1d is a schematic representation of the surface displacement of one of the five $(t,1,2,m)$ modes. The frequencies of all torsional modes depend only on the transverse sound velocity, since they do not involve stretching displacements.

3. Brillouin and Raman scattering

The method for calculating the low frequency Raman/Brillouin spectrum of dielectric nanoparticles has been developed by Lamb (1881), Benassi *et al.* (1991), Mazzacurati *et al.* (1992), Montagna and Dusi (1995), Berne and Pecora (2000), and Montagna (2008a). The contribution of the p-th mode, with frequency ω^{p}, to the Stokes part of the spectrum can be put in the form (Benassi *et al.* 1991):

$$\begin{aligned} I^p_{\alpha\beta}(\mathbf{q}) &\propto \frac{n(\omega^p)+1}{\omega^p} \mid \sum_i e^{-i\mathbf{q}\cdot\mathbf{x}^i}[-i\mathbf{q}\cdot\mathbf{e}(i,p)\pi^i_{\alpha\beta} + Q^i_{\alpha\beta}] \mid^2 \\ &= \frac{n(\omega^p)+1}{\omega^p} C_{\alpha\beta}(\omega^p), \end{aligned} \tag{2}$$

where $n(\omega,T)$ is the Bose-Einstein factor, $C_{\alpha\beta}(\omega_{\mathrm{p}})$ is the mode-radiation coupling coefficient, α and β are the direction of polarization of the incident and scattered photon, respectively, $\hbar\omega = \hbar\omega_i - \hbar\omega_s$ and $\mathbf{q} = \mathbf{k}_i - \mathbf{k}_s$ are the exchanged energy and wavevector, respectively. $\pi^{\mathrm{i}}_{\alpha\beta}(t)$ is the effective microscopic polarizability tensor of the $i-$th scatterer at position $\mathbf{r}^{\mathrm{i}}(t)$,

$$\mathbf{r}^{\mathrm{i}}(t) = \mathbf{x}^{\mathrm{i}} + \mathbf{u}^{\mathrm{i}}(t), \tag{3}$$

where $\mathbf{u}^{\mathrm{i}}(t)$ is the displacement from the equilibrium position $\mathbf{x}^{\mathrm{i}}$. $\pi^{\mathrm{i}}_{\alpha\beta}(t)$ can be expanded in power series of the displacements $\mathbf{u}^{\mathrm{j}}$, and $\mathbf{u}^{\mathrm{i}}$ can be expressed in terms of the vibrational eigenvectors $\mathbf{e}(i,p)$, whose frequencies are ω_{p}:

$$\pi^{\mathrm{i}}_{\alpha\beta}(t) = \pi^{\mathrm{i}}_{\alpha\beta} + Q^{\mathrm{i}}_{\alpha\beta} \tag{4}$$

with

$$Q^{\mathrm{i}}_{\alpha\beta} = \sum_{\mathrm{j}}\sum_{\gamma} \frac{\partial \pi^{\mathrm{i}}_{\alpha\beta}}{\partial u^{\mathrm{j}}_{\gamma}}[e_\gamma(j,p) - e_\gamma(i,p)]. \tag{5}$$

$\pi^{\mathrm{i}}_{\alpha\beta}$ is the bare polarizability of the i-th unit and its derivatives with respect to the displacements of the surrounding atoms are calculated at the equilibrium position $\mathbf{x}^{\mathrm{i}}$. The first term, $-i\sum_i \pi^i_{\alpha\beta} e^{-i\mathbf{q}\cdot\mathbf{x}^i}\mathbf{q}\cdot\mathbf{e}(i,p)$, describes the polarization fluctuations due to the displacement of the units from their equilibrium position. It is called the Brillouin term (Montagna 2008a). The second term, $\sum_{\mathrm{i}} e^{-i\mathbf{q}\cdot\mathbf{x}^{\mathrm{i}}} Q^{\mathrm{i}}_{\alpha\beta}$, is due to two kinds of induced effects: i) the local field changes due to the motion of the surrounding dipoles (Dipole Induced Dipoles, DID); ii) the electronic polarizability changes with the change of the atomic distances (Bond Polarization, BP). This term is called Raman term (Montagna 2008a).

If the particle size d is much smaller than the wavelength of the exciting light, the mechanism of scattering due to density fluctuations is not active. Therefore, only the Raman term is active for small particles ($qd \ll 1$). No q-dependence is present, so that isotropic scattering is observed instead of the Bragg-like scattering, typical of systems which extend over many wavelengths.

Even if different assignments have been proposed (Kanehisa 2005, 2006; Li *et al.* 2007; Gupta *et al.* 2009), it has been shown that, on the basis of symmetry arguments, only the symmetric ($l=0$) and quadrupolar ($l=2$) spheroidal modes are Raman active (Duval 1992; Montagna and Dusi 1995; Goupalov *et al.* 2006; Montagna 2008b). The $l=0$ modes give a polarized (VV, vertical-vertical, parallel polarization in excitation and detection) Raman spectrum, whereas the $l=2$ modes give depolarized spectra, allowing one to distinguish the nature of the vibrations by a comparison of the VV and HV (horizontal-vertical, crossed polarizations) polarized spectra.

The physical mechanism of photon-phonon interaction depends on the system and determines the relative activity of the two sequences of vibrations. In metal particles, the $l=2$ vibrations dominate the Raman spectrum (Fujii *et al.* 1991; Palpant *et al.* 1999a,b; Bachelier and Mlayah 2004; Murray *et al.* 2007; Mankad *et al.* 2013; Girard *et al.* 2017). In dielectric particles, the quadrupolar modes or symmetric modes dominate the spectra when the DID or BP are more important, respectively (Mattarelli *et al.* 2006; Murray *et al.* 2007). This result explains why semiconductor nanoparticles with covalent bonds show intense symmetric scattering (Irmer *et al.* 2000; Huntzinger *et al.* 2006; Ivanda *et al.* 2006, 2007; Mankad *et al.* 2012), whereas fluoride crystals with ionic bond show Raman scattering from quadrupolar modes (Tikhomirov *et al.* 2002, 2003; Mattarelli *et al.* 2005), and why in oxide crystals, as titania, zirconia, and hafnia, the two modes show comparable Raman activity (Montagna *et al.* 2003; Jestin *et al.* 2006).

The Raman coupling coefficient, especially for the $l=0$ vibrations, is nearly the same for all the modes of a sequence, with different radial wavevector. However, the $[n(\omega)+1)]/\omega \sim 1/\omega^{-2}$ factor, due to the thermal averaging in harmonic approximation, determines a Raman spectrum with a sequence of peaks of decreasing intensity as the radial index n increases (Montagna and Dusi 1995). For this reason, only the first mode, $n=1$, of the $l=0$ and/or $l=2$ spheroidal vibrations is clearly observed in most systems. As an example, Fig. 2 shows the polarized spectra of a glass ceramic with nanoparticles of the cubic β-PbF_2 phase in a oxyfluoride glass. The sample was obtained by annealing the parent glass for 5 h at 440 °C (Montagna *et al.* 2003) The spectra were measured in a standard 90 degree geometrical configuration, by exciting the samples with the 514.5 nm line of an Ar^+-ion laser. A double monochromator with a 2 m focal length and gratings with 300 lines/mm, working at the eleventh order, was employed. The high transparency of the glass ceramics allows to have a quite small contribution of the elastic line in the very low frequency region (Mattarelli *et al.* 2007, 2010).

The sharp peak at 0.7 cm^{-1}, with a linewidth given by the resolution of about 0.13 cm^{-1}, is the Brillouin peak due to the longitudinal phonons of the glass ceramic. Its intensity has been reduced by a factor 5 in the VV spectrum and by a factor of five in the HV spectrum. The depolarized (*i.e.*, present both in VV and HV spectra) band centered at about 2.8 cm^{-1} and the broader polarized (present almost exclusively in the VV spectrum) band, appearing as a shoulder at about 6 cm^{-1}, are attributed to the $(s,1,2)$ and $(s,1,0)$ modes of the nanoparticles. A nearly constant background with intensity comparable to that of the peaks is the vibrational contribution of the glass, the low frequency tail of an intense Boson peak. The large width of the $(s,1,2)$ band has two physical causes. The first is the size dispersion of the particles that causes inhomogeneous line broadening. The second is the interaction of the nanoparticles with the surrounding glass that causes homogeneous

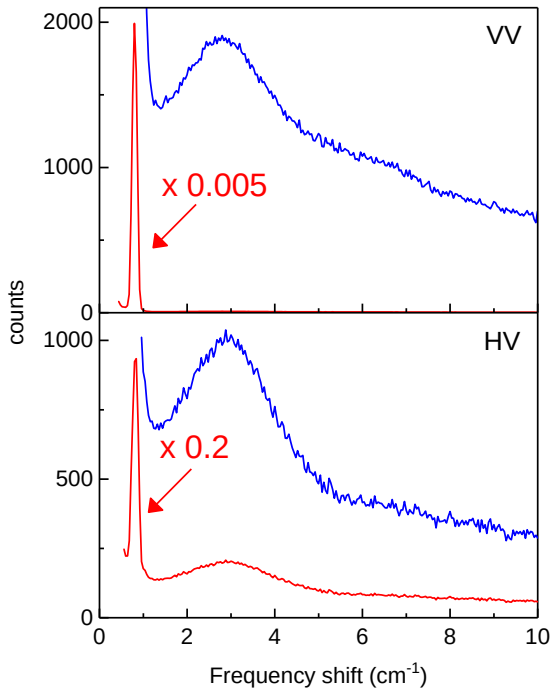

FIGURE 2. VV and HV polarized Raman and Brillouin spectra of a glass ceramic made of an oxyfluoride glass containing β-PbF_2 nanocrystals (red lines). Integration time is 6 s. The spectra are shown in two intensity scales with the indicated ratio.

line broadening (Montagna and Dusi 1995; Zi *et al.* 1998; Saviot *et al.* 2004): vibrations are no more confined in the sphere, but extend into the glass medium. A model that considers the two source of broadening, taking a log-normal distribution of particle sizes, allows to reproduce the spectral patterns providing the values of the mean size and width of the distribution. The model is applied to the lineshape of the $(s,1,2)$ peak in the HV spectrum, since the $l = 0$ vibrations are Raman active only in VV polarization. The fit gives a mean size of about 14 nm with a sharp size distribution, 2 nm at full width half maximum, the main contribution to the observed much larger linewidth being due to homogeneous line broadening.

The applicability of the simple Lamb model for a homogeneous medium to the case of an anisotopic spherical crystal has been studied by Saviot *et al.* (2004). The anisotropy results

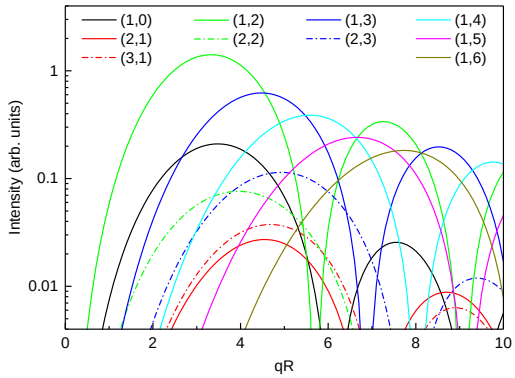

FIGURE 3. Calculated BS intensities for the lowest frequency spheroidal modes of PS particles.

in a splitting of the $l = 2$ mode for spherical Si nanocrystals. However, this study shows that the use of the Lamb model is still a good approximation. Few studies has been carried out on core-shell particles (Still *et al.* 2008; Ristic *et al.* 2009; Sun *et al.* 2010; Mork *et al.* 2016; Lee *et al.* 2017), and on particles with non-spherical shapes, as cubic, octahedral particles (Sun *et al.* 2010; Pan *et al.* 2011), nanorods and nanowires (Saviot 2018). Finally, it should be mentioned some measurements performed on organic materials, such as viruses (Karpova *et al.* 2016; Tcherniega *et al.* 2018) and proteins (Shevchenko *et al.* 2019).

All the results presented above, except possibly the last ones, were obtained for small particles showing only $l = 0$ and $l = 2$ spheroidal modes. On the contrary, for particles with a size comparable to the wavelength of the light, all spheroidal (s,n,l,m) become active. The Brillouin term, which produces VV polarized spectra, becomes dominant over the Raman one that should allow to participate all modes, including the torsional ones, in VH polarization (Montagna 2008b). As a matter of fact, a contribution from torsional modes has never been observed. The scattering is q-dependent. The number of peaks appearing in the Brillouin spectra increases as the particle size and q increases. This is shown in Fig. 3, where the calculated intensities of the lowest frequency (s,n,l) modes are reported, as a function of the adimensional quantity qR ($R = d/2$), for particles with $v_L/v_T = 1.99$, a value suitable for polystyrene (PS) particles. The index s has been removed for graphical reasons.

Many dozen of peaks can be observed for particles with a diameter larger than 500 nm. Figure 4 shows the single contribution of the lowest frequency (s,n,l) modes and their sum, calculated for a PS sphere with d=550 nm. This calculated spectrum, broadened for accounting of the limited experimental resolution, is compared in Fig. 5 with the experimental spectrum, partially already reported in Fig. 6 (with reduced scales) (Mattarelli *et al.* 2012).

It is important to note that, even if the Brillouin scattering is q-dependent (the intensity of the peaks are q-dependent, not the frequencies of the confined vibration, that are determined

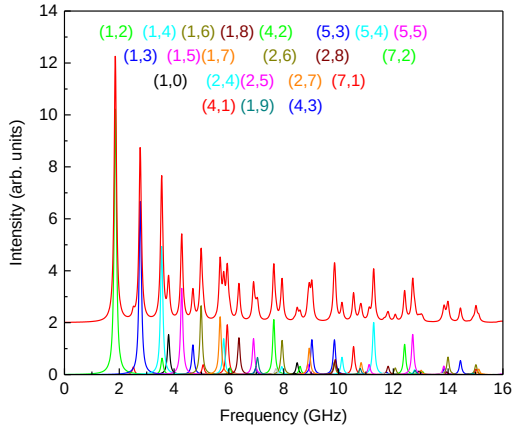

FIGURE 4. Calculated BS spectrum with contributions from the lowest frequency modes of a 550 nm PS particle.

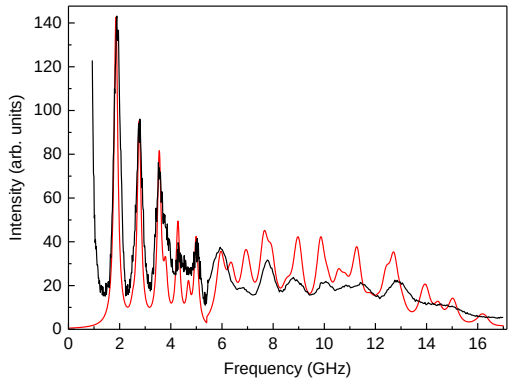

FIGURE 5. Comparison of the experimental (black line) and calculated (red line) BS spectrum of a 550 nm PS particle.

by the size and the mechanical structure), this q-dependency is masked by multiple scattering occurring in partially opaque samples of thick clusters of particles. Contributions of all exchanged q-values, from zero to the backscattering one, $q_{\mathrm{BS}} = 2k_{\mathrm{i}} = 4\pi n/\lambda$, where n is the refractive index, appear at any angle of measurement (Still *et al.* 2010). The calculated intensities account for this by taking the sum of the scattering intensities at all q-values. Figure 6 shows the result of this calculation. For small qR, the $(s,1,2)$ peak is largely dominant. As qR increases, more and more different (s,n,l) modes become important.

The calculation of Fig. 4 can reproduce the main features of the Brillouin spectra, but it is evident that a refinement of the theoretical approach is needed to reproduce the relative

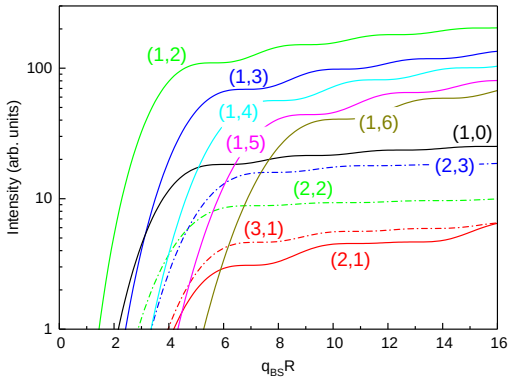

FIGURE 6. Calculated BS intensities for the lowest frequency modes of PS particles by summing over all exchanged $0 < q \leq q_{\mathrm{BS}}$.

intensities and the finite width of the lines. We must consider that particles are not isolated, but interact in the cluster with forces at their contacts.

4. fcc crystals of spheres

When two spheres approach, the molecular forces of attraction produce a deformation which appears as a circular area of contact. The strain pattern in the region of contact is complex, with repulsive forces with compressive strains in the central region and attractive forces with tensile strains in the external region of the contact circle. According to the JFK model, for a small interaction, two spheres with diameter d have a circular contact area of radius a_0 in case of no external force (Johnson *et al.* 1971):

$$a_0 = (\frac{3\pi d^2 W_a}{8K})^{1/3} \propto d^{2/3}, \tag{6}$$

where W_{a} is the surface energy and K is the bulk elastic modulus. The interaction between two spheres can be described by a spring constant normal to the contact surface given by

$$k_n = B W_a^{1/3} d^{2/3} K^{1/3} \propto d^{2/3}, \tag{7}$$

where the dimensionless quantity B depends on the model assumed for the distribution of the strains in the contact volume (Mattarelli *et al.* 2013). The most important things are the scaling laws, $a_0 \propto d^{2/3}$ and $k_n \propto d^{2/3}$, since they provide the size dependence of the effects of the interaction.

Usually, the clusters of nanoparticles are poly-crystals of fcc structure as in Fig. 7, where a picture at the optical microscope is shown for particles with $d = 2$ mm. Smaller particles can be observed in the pictures taken by scanning electron microscopy (Kim *et al.* 2018).

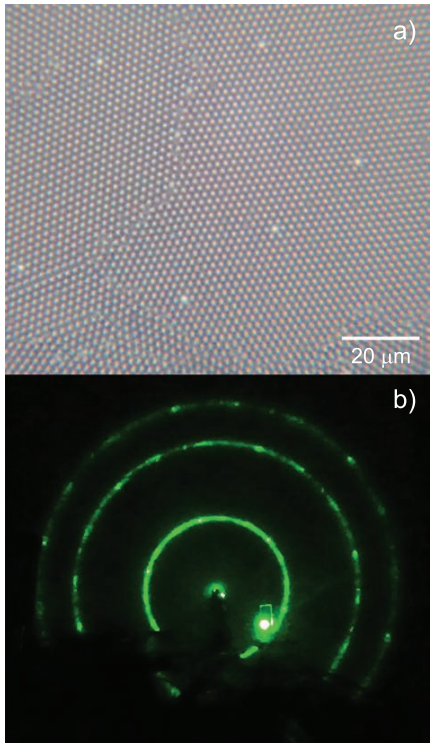

FIGURE 7. Optical microscope picture of a polycrystalline cluster of PS particles with $d = 2\ \mu m$. The hexagonal structure is that of the (111) surface of a fcc crystal. Diffraction pattern of a laser beam with $\lambda = 543$ nm and a diameter of 2 mm. Crystals with different orientation produce groups of six spots arranged in ring.

A perfect fcc crystal, even in the presence of some degree of disorder, is a good model for studying the effect of the interaction among particles. Two main new effects appear. The first is that each discrete (p,n,l,m) mode of the isolated sphere becomes a phonon band with dispersion larger as the interaction among the spheres is larger. The second is that the symmetry is lowered from the spherical one to that of a phonon with a defined q-vector. Even at the gamma point, $q = 0$ with all spheres moving in phase, the symmetry is lowered from spherical to cubic. The $2l+1$ degeneration is at least partially resolved and crystal phonons deriving from different (p,n,l,m) modes of the sphere, but having the same crystal symmetry, can mix.

Figures 8 and 9 show the dispersion curves along a low symmetry (124) direction for few low frequency modes. The Brillouin zone border (BZB) in this direction is a little bit smaller than the maximum $q_X = \sqrt{2}\pi/d$ in the (100) direction. The calculation has been done by connecting nearly spherical finite clusters of masses by few springs in the contact region (Mattarelli *et al.* 2013).

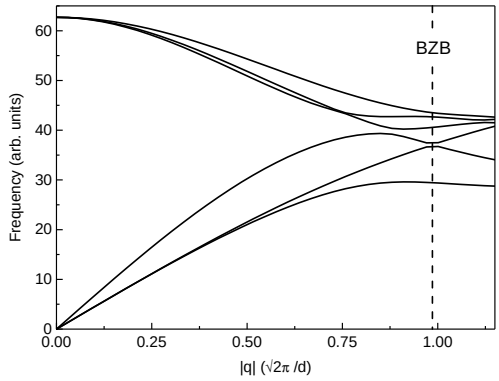

FIGURE 8. Calculated dispersion curves for the $(s,1,1)$ and $(t,1,1)$ phonon bands along the (1,2,4) direction. The dashed vertical line indicate the Brillouin zone border for this direction

The three lower curves of Fig. 8 describe the two transverse and the longitudinal sound propagation in the crystal. They derive from the three degenerate $(s,1,1)$ mode of the single particle, a zero frequency mode of rigid translation of the whole sphere. The sound propagates through the spheres maintaining nearly rigid structures with strains appearing only in a small region at the contacts. In an ideal fcc crystal, the maximum vibrational frequency, for waves propagating along the [100] directions, is

$$\omega_{\max} = 2\sqrt{K_{\text{eff}}/M} \propto d^{-7/6} \tag{8}$$

where M is the mass of the sphere and the scaling laws with the particle size, *i.e.*, $K_{eff} \propto k_{\text{n}} \propto d^{2/3}$ and $M \propto d^3$, have been used. In this regime, the longitudinal sound velocity of the system scales as

$$v_{\text{L}} \propto d\sqrt{K_{\text{eff}}/M} \propto d^{-1/6} \tag{9}$$

These theoretical expectations have been confirmed in BS experiments on PS clusters. The observable quantity is the broad low frequency band appearing at frequencies lower than that of the lowest frequency $(s,1,2)$ peak, attributed to the full density of longitudinal sound waves. The high frequency tail of this band presents a scaling law with the particle size well reproduced by Eq. (8) (Mattarelli and Montagna 2012; Kim *et al.* 2018). The simple model described above appears to work well. Therefore, we can deduce that the effect of the interaction is relatively more important for small particles. In particular, the deformation from the spherical shape that can be measured by $a_0/d \propto d^{-1/3}$ and the sound velocity $v_{\text{L}} \propto d^{-1/6}$ increase with decreasing the particle size.

The three upper dispersion curves of Fig. 8 derive from the $(t,1,1)$ modes, the three zero frequency pure rotation of the free sphere. It should be noted that translation and

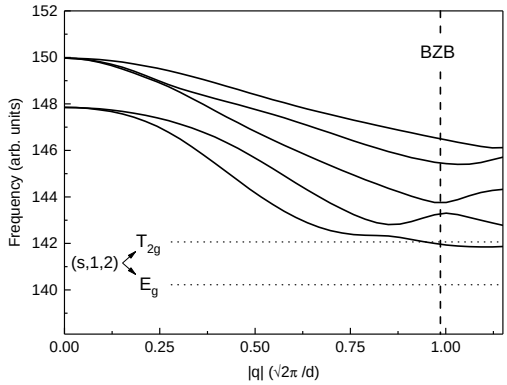

FIGURE 9. Calculated dispersion curves for the $(s,1,2)$ phonon band along the (1,2,4) direction.

rotation modes mix near the zone border, where they have close frequency since the relative displacement of two counter-rotating spheres produces the same strain at the contact as the counter-translation.

Figure 9 shows the dispersion curves for the $(s,1,2)$ vibrations. Here, and in all higher frequency modes, the dispersion is less effective than for the $(s,1,1)$ and $(t,1,1)$, very sensitive to the interaction since are zero-frequency modes in the free particle. The DOS of the $(s,1,2)$ band is centered at a frequency higher than the relative frequency of the free particle. This is true for all phonon band, since any constrain to a free vibration increases its frequency. The frequency of the free $(s,1,2)$ vibrations are indicated by the horizontal dotted lines. Here, the $2l+1=5$ multiplet is split in a triplet and a doublet, since the numerical calculation is not done on a spherical particle, but on a finite cluster, with a symmetry lowered to cubic. The width of the DOS is comparable with the shift toward higher frequency of the band center of mass, and both width and shift are nearly linear with the interaction, for small k_{eff}. This observation allows to estimate from the shape of the observed $(s,1,2)$ band two important quantities: i) the frequency of the free sphere, which gives information on the mechanical properties of the particles; ii) the strength of the interaction, which governs the propagation of the sound waves and all other phonons in the crystal of particles. A study on cluster of PS particles of different size and chemical composition, has recently shown that the mechanical properties of the particles are independent on the size, but depend on the chemical route used to produce the particles. In particular, harder particles can be obtained by adding cross-linkers (Kim *et al.* 2018). On the other hand, the effect of the interaction seems to scale with the particle size as predicted by the scaling laws of Eqs. 5-8 with no evident dependence on the different chemical processes for producing the particles.

5. Temperature-dependent particle vibrational modes and interaction.

When the temperature is increased from room temperature towards T_g, the particles progressively collapse to form a compact film. There is a regime for a large interval of T, in which the Brillouin spectra show a shift towards low frequency of all peaks. The effect is reversible and can be attributed to anharmonicity that softens the glass. This occurs up to a temperature T_x, over which an opposite shift is observed with a progressive broadening of all bands. The smaller the size of the particles, the smaller the temperature T_x at which this inversion occurs. Therefore, there is a temperature interval, lower than T_g where the particles progressively collapse by progressively increasing the size of the contact region. This increases the strength of the interaction producing high frequency shift and broadening of all (p,n,l) phonon bands. The final collapse into a compact film, observed by the disappearance of the particle vibrations and the appearance of the Brillouin peak of a homogeneous glass, occurs at the the same temperature, T_g, independent on both the chemical route and the particle size. The observation of a size dependent T_x suggests the existence of a surface mobile layer atop the NP and therefore a gradient in the dynamics of polymer chains approaching T_g, as already suggested on the basis of thermal measurements (Sasaki *et al.* 2003; Zhang *et al.* 2011; Feng *et al.* 2013; Martinez-Tong *et al.* 2013; Christie *et al.* 2016; Perez-de-Eulate *et al.* 2017). Such a softer surface layer will have a larger effect in smaller particles, where it will occupy a larger volume fraction.

6. Conclusions

The inelastic light scattering by spherical particles in a wide range of sizes, from few nanometers to micrometers are reviewed. Two different physical mechanisms are at the source of the scattering. For small particles ($d \lesssim 20$ nm), the Raman scattering dominates, and few peaks appear in the spectra. For large particles ($d \gtrsim 80$ nm), the Brillouin scattering dominate and many peaks are observed. The inelastic light scattering experiments give information on the mechanical properties of the particles and on the interaction among particles in clusters, as in phononic crystals, or with a surrounding medium of isolated particles, as in glass ceramics. Recent results show that nano-confinement affects the mechanical properties and the dynamics at temperatures near to the glass temperature of the bulk material.

References

Abel, H.-B. (1990). "Low-frequency SERS from Ag colloids in alkali halide crystals". *Physica Status Solidi (b)* **161**(1), 435–445. DOI: 10.1002/pssb.2221610144.

Bachelier, G., Margueritat, J., Mlayah, A., Gonzalo, J., and Afonso, C. N. (2007). "Size dispersion effects on the low-frequency Raman scattering of quasispherical silver nanoparticles: Experiment and theory". *Physical Review B* **76** (23), 235419–235424. DOI: 10.1103/PhysRevB.76.235419.

Bachelier, G. and Mlayah, A. (2004). "Surface plasmon mediated Raman scattering in metal nanoparticles". *Physical Review B* **69** (20), 205408–205414. DOI: 10.1103/PhysRevB.69.205408.

Benassi, P., Pilla, O., Mazzacurati, V., Montagna, M., Ruocco, G., and Signorelli, G. (1991). "Disorder-induced light scattering in solids: Microscopic theory and applications to some model systems". *Physical Review B* **44**(21), 11734–11742. DOI: 10.1103/PhysRevB.44.11734.

Berne, B. J. and Pecora, R. (2000). *Dynamic Light Scattering: With Applications to Chemistry, Biology, and Physics*. Dover Books on Physics Series. Dover Publications.

Bottani, C. E., Bassi, A. L., Stella, A., Cheyssac, P., and Kofman, R. (2001). "Investigation of confined acoustic phonons of tin nanoparticles during melting". *Europhysics Letters (EPL)* **56**(3), 386–392. DOI: 10.1209/epl/i2001-00531-8.

Bragas, A. V., Aku-Leh, C., and Merlin, R. (2006). "Raman and ultrafast optical spectroscopy of acoustic phonons in $CdTe_{0.68}Se_{0.32}$ quantum dots". *Physical Review B* **73** (12), 125305–125310. DOI: 10.1103/PhysRevB.73.125305.

Capobianco, J. A., Proulx, P. P., Andrianasolo, B., and Champagnon, B. (1991). "Nucleation kinetic studies of a europium-doped aluminosilicate glass: Low-frequency inelastic scattering and fluorescence line narrowing". *Physical Review B* **43**(13, A), 10031–10035. DOI: 10.1103/PhysRevB.43.10031.

Cataliotti, R. S., Compagnini, G., Morresi, A., Ombelli, M., and Sassi, P. (2002). "Polarization properties of low frequency inelastic scattering by acoustic phonons in gold nanoclusters". *Physical Chemistry Chemical Physics* **4**(12), 2774–2779. DOI: 10.1039/b110225g.

Ceccato, R., Dal Maschio, R., Gialanella, S., Mariotto, G., Montagna, M., Rossi, F., Ferrari, M., Lipinska-Kalita, K. E., and Ohki, Y. (2001). "Nucleation of Ga_2O_3 nanocrystals in the K_2O-Ga_2O_3-SiO_2 glass system". *Journal of Applied Physics* **90**(5), 2522–2527. DOI: 10.1063/1.1365426.

Champagnon, B., Andrianasolo, B., Ramos, A., Gandais, M., Allais, M., and Benoit, J.-P. (1993). "Size of Cd(S,Se) quantum dots in glasses: Correlation between measurements by high-resolution transmission electron microscopy, small-angle X-ray scattering, and low-frequency inelastic Raman scattering". *Journal of Applied Physics* **73**(6), 2775–2780. DOI: 10.1063/1.353053.

Champagnon, B., Boukenter, A., Duval, E., Mai, C., Vigier, G., and Rodek, E. (1987). "Early stages of nucleation of Zerodur glass. Very low frequency Raman scattering and small angle X-ray scattering investigations". *Journal of Non Crystalline Solids* **94**(2), 216–221. DOI: 10.1016/S0022-3093(87)80291-0.

Chen, I. C., Weng, C.-L., Lin, C.-H., and Tsai, Y.-C. (2010). "Low-frequency Raman scattering from acoustic vibrations of spherical CdSe/CdS nanoparticles". *Journal of Applied Physics* **108**(8), 083530–9. DOI: 10.1063/1.3499651.

Christie, D., Zhang, C., Fu, J., Koel, B., and Priestley, R. D. (2016). "Glass transition temperature of colloidal polystyrene dispersed in various liquids". *Journal of Polymer Science Part B: Polymer Physics* **54**(17), 1776–1783. DOI: 10.1002/polb.24082.

Duval, E. (1992). "Far-infrared and Raman vibrational transitions of a solid sphere: Selection rules". *Physical Review B* **46**(9), 5795–5797. DOI: 10.1103/PhysRevB.46.5795.

Duval, E., Boukenter, A., and Champagnon, B. (1986). "Vibration Eigenmodes and Size of Microcrystallites in Glass: Observation by Very-Low-Frequency Raman Scattering". *Physical Review Letters* **56**(19), 2052–2055. DOI: 10.1103/PhysRevLett.56.2052.

Duval, E., Portales, H., Saviot, L., Fujii, M., Sumitomo, K., and Hayashi, S. (2001). "Spatial coherence effect on the low-frequency Raman scattering from metallic nanoclusters". *Physical Review B* **63**(7), 075405–075410. DOI: 10.1103/PhysRevB.63.075405.

Feng, S., Li, Z., Liu, R., Mai, B., Wu, Q., Liang, G., Gao, H., and Zhu, F. (2013). "Glass transition of polystyrene nanospheres under different confined environments in aqueous dispersions". *Soft Matter* **9**(18), 4614–4620. DOI: 10.1039/c3sm27576k.

Ferrari, M., Gonella, F., Montagna, M., and Tosello, C. (1996). "Detection and size determination of Ag nanoclusters in ion-exchanged soda-lime glasses by waveguided Raman spectroscopy". *Journal of Applied Physics* **79**(4), 2055–2059. DOI: 10.1063/1.361060.

Fujii, M., Kanzawa, Y., Hayashi, S., and Yamamoto, K. (1996). "Raman scattering from acoustic phonons confined in Si nanocrystals". *Physical Review B* **54**(12), R8373–R8376. DOI: 10.1103/PhysRevB.54.R8373.

Fujii, M., Nagareda, T., Hayashi, S., and Yamamoto, K. (1991). "Low-frequency Raman scattering from small silver particles embedded in SiO_2 thin films". *Physical Review B* **44**(12), 6243–6248. DOI: 10.1103/PhysRevB.44.6243.

Gangopadhyay, P., Kesavamoorthy, R., Nair, K. G. M., and Dhandapani, R. (2000). "Raman scattering studies on silver nanoclusters in a silica matrix formed by ion-beam mixing". *Journal of Applied Physics* **88**(9), 4975–4979. DOI: 10.1063/1.1290739.

Girard, A., Lerme, J., Gehan, H., Margueritat, J., and Mermet, A. (2017). "Mechanisms of resonant low frequency Raman scattering from metallic nanoparticle Lamb modes". *The Journal of Chemical Physics* **146**(19), 194201. DOI: 10.1063/1.4983119.

Goupalov, S. V., Saviot, L., and Duval, E. (2006). "Comment on "Infrared and Raman selection rules for elastic vibrations of spherical nanoparticles"". *Physical Review B* **74**(19), 197401. DOI: 10.1103/PhysRevB.74.197401.

Gupta, S. K., Jha, P. K., and Arora, A. K. (2008). "Size dependent acoustic phonon dynamics of $CdTe_{0.68}Se_{0.32}$ nanoparticles in borosilicate glass". *Journal of Applied Physics* **103**(12), 124307. DOI: 10.1063/1.2943271.

Gupta, S. K., Sahoo, S., Jha, P. K., Arora, A. K., and Azhniuk, Y. M. (2009). "Observation of torsional mode in $CdS_{1-x}Se_x$ nanoparticles in a borosilicate glass". *Journal of Applied Physics* **106**(2), 024307. DOI: 10.1063/1.3171925.

Huntzinger, J.-R., Mlayah, A., Paillard, V., Wellner, A., Combe, N., and Bonafos, C. (2006). "Electron-acoustic-phonon interaction and resonant Raman scattering in Ge quantum dots: Matrix and quantum confinement effects". *Physical Review B* **74**(11), 115308. DOI: 10.1103/PhysRevB.74.115308.

Irmer, G., Monecke, J., Verma, P., Goerigk, G., and Herms, M. (2000). "Size analysis of nanocrystals in semiconductor doped silicate glasses with anomalous small-angle X-ray and Raman scattering". *Journal of Applied Physics* **88**(4), 1873–1879. DOI: 10.1063/1.1305462.

Ivanda, M., Babocsi, K., Dem, C., Schmitt, M., Montagna, M., and Kiefer, W. (2003). "Low-wave-number Raman scattering from CdS_xSe_{1-x} quantum dots embedded in a glass matrix". *Physical Review B* **67**(23), 235329. DOI: 10.1103/PhysRevB.67.235329.

Ivanda, M., Gebavi, H., Ristic, D., Furic, K., Music, S., Ristic, M., Zonja, S., Biljanovic, P., Gamulin, O., Balarin, M., Montagna, M., Ferrari, M., and Righini, G. C. (2007). "Silicon nanocrystals by thermal annealing of Si-rich silicon oxide prepared by the LPCVD method". *Journal of Molecular Structure* **834**, 461–464. DOI: 10.1016/j.molstruc.2006.09.036.

Ivanda, M., Hohl, A., Montagna, M., Mariotto, G., Ferrari, M., Orel, Z. C., Turkovic, A., and Furic, K. (2006). "Raman scattering of acoustical modes of silicon nanoparticles embedded in silica matrix". *Journal of Raman Spectroscopy* **37**(1-3), 161–165. DOI: 10.1002/jrs.1445.

Ivanda, M., Music, S., Gotic, M., Turkovic, A., Tonejc, A. M., and Gamulin, O. (1999). "The effects of crystal size on the Raman spectra of nanophase TiO_2". *Journal of Molecular Structure* **481**, 641–644. DOI: 10.1016/s0022-2860(98)00921-1.

Jestin, Y., Afify, N., Armellini, C., Berneschi, S., Bhaktha, S. N. B., Boulard, B., Chiappini, A., Chiasera, A., Dalba, G., Duverger, C., Ferraria, M., Lopez, C. E. G., Mattarelli, M., Montagna, M., Moser, E., Conti, G. N., Pellic, S., Righini, G. C., and Rocca, F. (2006). "Er^{3+}-activated silica-hafnia glass-ceramics planar waveguides - art. no. 61831W". In: *Integrated Optics, Silicon Photonics, and Photonic Integrated Circuits*. Ed. by G. Righini. Vol. 6183. Proceedings of SPIE-The International Society for Optical Engineering. Conference on Integrated Optics, Silicon Photonics, and Photonic Integrated Circuits, Strasbourg, FRANCE, APR 03-05, 2006, W1831. DOI: 10.1117/12.664610.

Johnson, K. L., Kendall, K., and Roberts, A. D. (1971). "Surface energy and the contact of elastic solids". *Proceedings of the Royal Society of London. A. Mathematical and Physical Sciences* **324**(1558), 301–313. DOI: 10.1098/rspa.1971.0141.

Kanehisa, M. (2005). "Infrared and Raman selection rules for elastic vibrations of spherical nanoparticles". *Physical Review B* **72** (24), 241405. DOI: 10.1103/PhysRevB.72.241405.

Kanehisa, M. (2006). "Reply to "Comment on 'Infrared and Raman selection rules for elastic vibrations of spherical nanoparticles' "". *Physical Review B* **74** (19), 197402. DOI: 10.1103/PhysRevB.74.197402.

Karpova, O. V., Kudryavtseva, A. D., Lednev, V. N., Mironova, T. V., Oshurko, V. B., Pershin, S. M., Petrova, E. K., Tcherniega, N. V., and Zemskov, K. I. (2016). "Stimulated low-frequency Raman scattering in a suspension of tobacco mosaic virus". *Laser Physics Letters* **13**(8), 085701. DOI: 10.1088/1612-2011/13/8/085701.

Kim, H., Cang, Y., Kang, E., Graczykowski, B., Secchi, M., Montagna, M., Priestley, R. D., Furst, E. M., and Fytas, G. (2018). "Direct observation of polymer surface mobility via nanoparticle vibrations". *Nature Communications* **9**. DOI: 10.1038/s41467-018-04854-w.

Kostic, R., Askrabic, S., Dohcevic-Mitrovic, Z., and Popovic, Z. V. (2008). "Low-frequency Raman scattering from CeO_2 nanoparticles". *Applied Physics A-Materials Science & Processing* **90**(4), 679–683. DOI: 10.1007/s00339-007-4345-6.

Kuok, M. H., Lim, H. S., Ng, S. C., Liu, N. N., and Wang, Z. K. (2003a). "Brillouin study of the quantization of acoustic modes in nanospheres". *Physical Review Letters* **90**(25), 255502. DOI: 10.1103/PhysRevLett.90.255502.

Kuok, M. H., Lim, H. S., Ng, S. C., Liu, N. N., and Wang, Z. K. (2003b). "Erratum: Brillouin study of the quantization of acoustic modes in nanospheres [Physical Review Letters 90, 255502 (2003)]". *Physical Review Letters* **91**(14), 255502. DOI: 10.1103/PhysRevLett.91.149901.

Lamb, H. (1881). "On the vibrations of an elastic sphere". *Proceedings of the London Mathematical Society* **s1-13**(1), 189–212. DOI: 10.1112/plms/s1-13.1.189.

Lee, E. M. Y., Mork, A. J., Willard, A. P., and Tisdale, W. A. (2017). "Including surface ligand effects in continuum elastic models of nanocrystal vibrations". *The Journal of Chemical Physics* **147**(4), 044711. DOI: 10.1063/1.4995439.

Li, Y., Lim, H. S., Ng, S. C., and Kuok, M. H. (2007). "Selection rules for Raman scattering from eigenmodes of spherical nanoparticles". *Chemical Physics Letters* **440**(4-6), 321–323. DOI: 10.1016/j.cplett.2007.04.033.

Li, Y., Lim, H. S., Ng, S. C., Wang, Z. K., Kuok, M. H., Vekris, E., Kitaev, V., Peiris, F. C., and Ozin, G. A. (2006). "Micro-Brillouin scattering from a single isolated nanosphere". *Applied Physics Letters* **88**(2), 023112. DOI: 10.1063/1.2164924.

Malinovsky, V. K., Novikov, V. N., Sokolov, A. P., and Dodonov, V. G. (1988). "Low-frequency Raman scattering on surface vibrational modes of microcrystals". *Solid State Communications* **67**(7), 725–729. DOI: 10.1016/0038-1098(88)91015-0.

Mankad, V., Gupta, S. K., Jha, P. K., Ovsyuk, N. N., and Kachurin, G. A. (2012). "Low-frequency Raman scattering from Si/Ge nanocrystals in different matrixes caused by acoustic phonon quantization". *Journal of Applied Physics* **112**(5), 054318. DOI: 10.1063/1.4747933.

Mankad, V., Jha, P. K., and Ravindran, T. R. (2013). "Probing confined acoustic phonons in free standing small gold nanoparticles". *Journal of Applied Physics* **113**(7), 074303. DOI: 10.1063/1.4792654.

Mariotto, G., Montagna, M., Viliani, G., Duval, E., Lefrant, S., Rzepka, E., and Mai, C. (1988). "Low-energy Raman scattering from silver particles in alkali halides". *Europhysics Letters* **6**(3), 239–243. DOI: 10.1209/0295-5075/6/3/009.

Martinez-Tong, D. E., Soccio, M., Sanz, A., Garcia, C., Ezquerra, T. A., and Nogales, A. (2013). "Chain arrangement and glass transition temperature variations in polymer nanoparticles under 3D-confinement". *Macromolecules* **46**(11), 4698–4705. DOI: 10.1021/ma400379a.

Mattarelli, M., Gasperi, G., Montagna, M., and Verrocchio, P. (2010). "Transparency and long-ranged fluctuations: The case of glass ceramics". *Physical Review B* **82**(9). DOI: 10.1103/PhysRevB.82.094204.

Mattarelli, M. and Montagna, M. (2012). "Comment on 'Selection rules for Brillouin light scattering from eigenvibrations of a sphere' [Chemical Physical Letters 461 (2008) 111]". *Chemical Physics Letters* **524**, 112–115. DOI: 10.1016/j.cplett.2011.12.027.

Mattarelli, M., Montagna, M., Rossi, F., Chiasera, A., and Ferrari, M. (2006). "Mechanism of low-frequency Raman scattering from the acoustic vibrations of dielectric nanoparticles". *Physical Review B* **74**(15), 153412. DOI: 10.1103/PhysRevB.74.153412.

Mattarelli, M., Montagna, M., Rossi, F., Ferrari, M., Tikhomirov, V. K., and Seddon, A. B. (2005). "Tm^{3+}-activated transparent oxyfluoride glass ceramics: A study by Raman scattering of the nanocrystal size distribution". *Glass Physics and Chemistry* **31**(4), 519–524. DOI: 10.1007/s10720-005-0092-y.

Mattarelli, M., Montagna, M., Still, T., Schneider, D., and Fytas, G. (2012). "Vibration spectroscopy of weakly interacting mesoscopic colloids". *Soft Matter* **8**(15), 4235–4243. DOI: 10.1039/c2sm07034k.

Mattarelli, M., Montagna, M., and Verrocchio, P. (2007). "Ultratransparent glass ceramics: The structure factor and the quenching of the Rayleigh scattering". *Applied Physics Letters* **91**(6), 061911. DOI: 10.1063/1.2768642.

Mattarelli, M., Secchi, M., and Montagna, M. (2013). "Phononic crystals of spherical particles: A tight binding approach". *The Journal of Chemical Physics* **139**(17), 174710. DOI: 10.1063/1.4828436.

Mazzacurati, V., Montagna, M., Pilla, O., Viliani, G., Ruocco, G., and Signorelli, G. (1992). "Vibrational dynamics and Raman scattering in fractals: A numerical study". *Physical Review B* **45**(5), 2126–2137. DOI: 10.1103/PhysRevB.45.2126.

Mikac, L., Ivanda, M., Stefanic, G., Music, S., Furic, K., and Tonejc, A. M. (2011). "Spherical vibrational modes of ZrO_2-CuO nanoparticles". *Journal of Molecular Structure* **993**(1-3), 198–202. DOI: 10.1016/j.molstruc.2011.02.032.

Mohapatra, S., Mishra, Y. K., Warrier, A. M., Philip, R., Sahoo, S., Arora, A. K., and Avasthi, D. K. (2012). "Plasmonic, low-frequency Raman, and nonlinear optical-limiting studies in copper-silica nanocomposites". *Plasmonics* **7**(1), 25–31. DOI: 10.1007/s11468-011-9271-y.

Montagna, M. (2008a). "Brillouin and Raman scattering from the acoustic vibrations of spherical particles with a size comparable to the wavelength of the light". *Physical Review B* **77**(4), 045418. DOI: 10.1103/PhysRevB.77.045418.

Montagna, M. (2008b). "Comment on "Infrared and Raman selection rules for elastic vibrations of spherical nanoparticles"". *Physical Review B* **77**(16), 167401. DOI: 10.1103/PhysRevB.77.167401.

Montagna, M. and Dusi, R. (1995). "Raman scattering from small spherical particles". *Physical Review B* **52**(14), 10080–10089. DOI: 10.1103/PhysRevB.52.10080.

Montagna, M., Moser, E., Visintainer, F., Ferrari, M., Zampedri, L., Martucci, A., Guglielmi, M., and Ivanda, M. (2003). "Nucleation of titania nanocrystals in silica titania waveguides". *Journal of Sol-Gel Science and Technology* **26**(1-3), 241–244. DOI: 10.1023/A:1020755200573.

Mork, A. J., Lee, E. M. Y., and Tisdale, W. A. (2016). "Temperature dependence of acoustic vibrations of CdSe and CdSe-CdS core-shell nanocrystals measured by low-frequency Raman spectroscopy". *Physical Chemistry Chemical Physics* **18**(41), 28797–28801. DOI: 10.1039/c6cp05683k.

Murray, D. B., Netting, C. H., Mercer, R. D., and Saviot, L. (2007). "Polarizability calculation of vibrating nanoparticles for intensity of low wavenumber Raman scattering". *Journal of Raman Spectroscopy* **38**(6), 770–779. DOI: 10.1002/jrs.1692.

Palpant, B., Portales, H., Saviot, L., Lerme, J., Prevel, B., Pellarin, M., Duval, E., Perez, A., and Broyer, M. (1999a). "Quadrupolar vibrational mode of silver clusters from plasmon-assisted Raman scattering". *Physical Review B* **60**(24), 17107–17111. DOI: 10.1103/PhysRevB.60.17107.

Palpant, B., Saviot, L., Lerme, J., Prevel, B., Pellarin, M., Duval, E., Perez, A., and Broyer, M. (1999b). "Plasmon-phonon coupling and resonant Raman scattering of silver clusters". *The European Physical Journal D* **9**(1-4), 585–589. DOI: 10.1007/s100530050505.

Pan, H. H., Wang, Z. K., Lim, H. S., Ng, S. C., Zhang, V. L., Kuok, M. H., Tran, T. T., and Lu, X. M. (2011). "Hypersonic confined eigenvibrations of gold nano-octahedra". *Applied Physics Letters* **98**(13), 133123. DOI: 10.1063/1.3574024.

Perez-de-Eulate, N. G., Di Lisio, V., and Cangialosi, D. (2017). "Glass transition and molecular dynamics in polystyrene nanospheres by fast scanning calorimetry". *ACS Macro Letters* **6**(8), 859–86. DOI: 10.1021/acsmacrolett.7b00484.

Ristic, D., Ivanda, M., and Furic, K. (2009). "Application of the phonon confinement model on the optical phonon mode of silicon nanoparticles". *Journal of Molecular Structure* **924**, 291–293. DOI: 10.1016/j.molstruc.2008.10.054.

Rzepka, E., Taurel, L., and Lefrant, S. (1981). "First-order Raman scattering induced by Na and Ag colloids in NaCl, NaBr and NaI". *Surface Science* **106**(1-3), 345–349. DOI: 10.1016/0039-6028(81)90221-1.

Sasaki, T., Shimizu, A., Mourey, T. H., Thurau, C. T., and Ediger, M. D. (2003). "Glass transition of small polystyrene spheres in aqueous suspensions". *The Journal of Chemical Physics* **119**(16), 8730–8735. DOI: 10.1063/1.1613257.

Saviot, L. (2018). "Vibrations of single-crystal gold nanorods and nanowires". *Physical Review B* **97**(15), 155420. DOI: 10.1103/PhysRevB.97.155420.

Saviot, L., Le Gallet, S., Demoisson, F., David, L., Sudre, G., Girard, A., Margueritat, J., and Mermet, A. (2017). "Inelastic light scattering contribution to the study of the onset of sintering of a nanopowder". *The Journal of Physical Chemistry C* **121**(4), 2487–2494. DOI: 10.1021/acs.jpcc.6b12280.

Saviot, L., Murray, D. B., and Lucas, M. D. M. de (2004). "Vibrations of free and embedded anisotropic elastic spheres: Application to low-frequency Raman scattering of silicon nanoparticles in silica". *Physical Review B* **69**(11). DOI: 10.1103/PhysRevB.69.113402.

Shevchenko, M. A., Chaikov, L. L., Kirichenko, M. N., Kudryavtseva, A. D., Mironova, T. V., Savichev, V. I., Sokovishin, V. V., Tcherniega, N. V., and Zemskov, K. I. (2019). "Stimulated low-frequency Raman scattering in albumin". *Journal of Russian Laser Research* **40**(1), 71–75. DOI: 10.1007/s10946-019-09771-x.

Simon, G., Meziane, L., Courty, A., Colomban, P., and Lisiecki, I. (2016). "Low wavenumber Raman scattering of cobalt nanoparticles self-organized in 3D superlattices far from surface plasmon resonance". *Journal of Raman Spectroscopy* **47**(2), 248–251. DOI: 10.1002/jrs.4782.

Still, T., Mattarelli, M., Kiefer, D., Fytas, G., and Montagna, M. (2010). "Eigenvibrations of submicrometer colloidal spheres". *The Journal of Physical Chemistry Letters* **1**(16), 2440–2444. DOI: 10.1021/jz100774b.

Still, T., Sainidou, R., Retsch, M., Jonas, U., Spahn, P., Hellmann, G. P., and Fytas, G. (2008). "The "Music" of core-shell spheres and hollow capsules: influence of the architecture on the mechanical properties at the nanoscale". *Nano Letters* **8**(10), 3194–3199. DOI: 10.1021/nl801500n.

Sun, J. Y., Wang, Z. K., Lim, H. S., Ng, S. C., Kuok, M. H., Tran, T. T., and Lu, X. (2010). "Hypersonic vibrations of $Ag@SiO_2$ (cubic core) - shell nanospheres". *ACS Nano* **4**(12), 7692–7698. DOI: 10.1021/nn102581g.

Tanaka, A., Onari, S., and Arai, T. (1993). "Low-frequency Raman-scattering from CdS microcrystals embedded in a germanium dioxide glass matrix". *Physical Review B* **47**(3), 1237–1243. DOI: 10.1103/PhysRevB.47.1237.

Tcherniega V, N., Pershin, S. M., Bunkin, A. F., Donchenko, E. K., Karpova V, O., Kudryavtseva, A. D., Lednev, V. N., Mironova V, T., Shevchenko, M. A., Strokov, M. A., and Zemskov I, K.

(2018). "Laser excitation of gigahertz vibrations in Cauliflower mosaic viruses' suspension". *Laser Physics Letters* **15**(9). DOI: 10.1088/1612-202X/aad28d.

Tikhomirov, V. K., Furniss, D., Seddon, A. B., Reaney, I. M., Beggiora, M., Ferrari, M., Montagna, M., and Rolli, R. (2002). "Fabrication and characterization of nanoscale, Er^{3+}-doped, ultratransparent oxy-fluoride glass ceramics". *Applied Physics Letters* **81**(11), 1937–1939. DOI: 10.1063/1.1497196.

Tikhomirov, V. K., Seddon, A. B., Ferrari, M., Montagna, M., Santos, L. F., and Almeida, R. M. (2003). "The structure of Er^{3+}-doped oxy-fluoride transparent glass-ceramics studied by Raman scattering". *Europhysics Letters* **64**(4), 529–535. DOI: 10.1209/epl/i2003-00106-9.

Verma, P., Gupta, L., Abbi, S. C., and Jain, K. P. (2000). "Confinement effects on the electronic and vibronic properties of $CdS_{0.65}Se_{0.35}$ nanoparticles grown by thermal annealing". *Journal of Applied Physics* **88**(7), 4109–4116. DOI: 10.1063/1.1289813.

Wu, X. L., Mei, Y. F., Siu, G. G., Wong, K. L., Moulding, K., Stokes, M. J., Fu, C. L., and Bao, X. M. (2001). "Spherical growth and surface-quasifree vibrations of Si nanocrystallites in Er-doped Si nanostructures". *Physical Review Letters* **86** (14), 3000–3003. DOI: 10.1103/PhysRevLett.86.3000.

Yang, Y. M., Wu, X. L., Yang, L. W., Huang, G. S., Siu, G. G., and Chu, P. K. (2005). "Low-frequency Raman scattering of Ge and Si nanocrystals in silica matrix". *Journal of Applied Physics* **98**(6), 064303. DOI: 10.1063/1.2035312.

Zatryb, G., Wilson, P. R. J., Wojcik, J., Misiewicz, J., Mascher, P., and Podhorodecki, A. (2015). "Raman scattering from confined acoustic phonons of silicon nanocrystals in silicon oxide matrix". *Physical Review B* **91**(23), 235444. DOI: 10.1103/PhysRevB.91.235444.

Zhang, C., Guo, Y., and Priestley, R. D. (2011). "Glass transition temperature of polymer nanoparticles under soft and hard confinement". *Macromolecules* **44**(10), 4001–4006. DOI: 10.1021/ma1026862.

Zhao, J. L. and Masumoto, Y. (1999). "Size dependence of confined acoustic phonons in CuCl nanocrystals". *Physical Review B* **60**(7), 4481–4484. DOI: 10.1103/PhysRevB.60.4481.

Zi, J., Zhang, K. M., and Xie, X. D. (1998). "Microscopic calculations of Raman scattering from acoustic phonons confined in Si nanocrystals". *Physical Review B* **58**(11), 6712–6715. DOI: 10.1103/PhysRevB.58.6712.

---

[a] Università degli Studi di Trento
Department of Industrial Engineering
via Sommarive 14, I-38123 Trento, Italy

[b] Università degli Studi di Trento
Department of Physics
via Sommarive 14, I-38123 Trento, Italy

* To whom correspondence should be addressed | email: montagna@science.unitn.it

Paper contributed to the international workshop entitled "Glasses and polymers: the science of disorder",
which was held in Messina, Italy (15–16 November 2018), under the patronage of the *Accademia Peloritana dei Pericolanti*
Manuscript received 21 May 2019; published online 1 October 2020